Composites Science and Technology 86 (2013) 142–148

Contents lists available at ScienceDirect

Composites Science and Technology

journal homepage: www.elsevier.com/locate/compscitech

Compressive strength and energy absorption of sandwich panels with aluminum foam-filled corrugated cores

L.L. Yan [a], B. Yu [a], B. Han [a], C.Q. Chen [b], Q.C. Zhang [a], T.J. Lu [a,*]

[a] State Key Laboratory for Mechanical Structure Strength and Vibration, Xi'an Jiaotong University, Xi'an 710049, PR China
[b] Department of Engineering Mechanics, CNMM, Tsinghua University, Beijing 100084, PR China

ARTICLE INFO

Article history:
Received 15 April 2013
Received in revised form 3 July 2013
Accepted 4 July 2013
Available online 26 July 2013

Keywords:
A. Sandwich
B. Mechanical properties
B. Strength/strain curves
C. Buckling

ABSTRACT

All-metallic corrugate core sandwich panels as primary loading structures may rapidly soften under compressive loading due mainly to core member buckling once the peak compressive stress is reached, resulting in reduced load-carrying capability. Inserting close-celled aluminum foam into the corrugate core has been envisioned as a feasible way to enhance the load capacity. The enhancement due to foam filling were firstly explored experimentally under quasi-static out-of-plane compression and the underlying mechanisms subsequently numerically studied using finite element simulations. The foam filled corrugated panel was found to have strength and energy absorption much greater than the sum of those of an empty corrugated sandwich panel and the aluminum foam alone. It was demonstrated that the core members in the foam-filled panel were considerably stabilized by the filling foam against lateral deflection. In particular, the elastoplastic buckling wavelength of the core members was significantly reduced and the transition from axial deformation to bending of the core member was much delayed, both of which contributing to the enhanced strength and energy adsorption capability of the foam filled panel.

1. Introduction

All-metallic sandwich panels with corrugated, pyramidal, Kagome and other periodic lattice cores have emerged as primary loading structures comparable with honeycomb sandwiches [1–5]. Under compressive loading, either quasi-static or dynamic, such panels usually reach their peak stress at a low strain and then soften rapidly due to node failure and/or core buckling. As a result, their load-carrying capability is rather limited. In contrast, the stress versus strain curve of cellular metallic foams fabricated by melt foaming route [6,7] exhibits a long plateau region, attractive for energy absorption in crushing and impulsive loading applications [7–11]. However, sandwich panels having metallic foam cores are considerably weaker in stiffness and strength due to the presence of a number of process-induced topological defects [12]. When a lattice-cored sandwich is subjected to intense pressure pulses, it is important that the core has both high crushing strength and high energy absorption per unit mass. It has been envisioned that this may be achieved if proper lateral support to core members against plastic yielding and buckling is supplied.

Metallic foams have already been used as a filling material to form foam-filled metallic tubes. It is inspiring that the foam filling could greatly increase the peak strength and energy absorption capacity to levels larger than the sum of those for the tube and the foam tested separately [13,14]. The enhancement was attributed to the reduced buckling wavelength of the tube during compressive stress by the filled foam. Studies on metallic foam filled thin walled sections [15] and polyurethane foams filled hexagonal cell aluminum honeycombs [16] also showed that foam filling could increase the strength and absorbed energy.

To stabilize core members against buckling so that the core may exhibit a sizable stress plateau analogous to that of metallic foams, low-density structural polymeric foams (Divinycell) were inserted into the interstices of metallic sandwich plates with folded plate cores (i.e., corrugated cores) to supply lateral support to the core members so that the buckling strength of these members may be enhanced [17,18]. The outcome was however disappointing, as sandwiches with polymeric foam-filled cores only performed nearly as well as sandwiches of the same weight with unfilled cores. Similarly disappointing results were obtained by filling polymeric foams into the interstices of metallic honeycomb sandwiches [16–18].

Instead of polymeric foams, the purpose of this study was to insert closed-cell aluminum foams into the core of steel sandwich panels and determine whether this was an effective approach to enhance the overall performance (peak compressive strength and energy absorption) of the sandwich when its total mass was constrained to be constant. Due to manufacturing advantages over square or hexagonal honeycomb cores, two-dimensional

* Corresponding author. Tel.: +86 29 8266 5600; fax: +86 29 8266 5937.
E-mail address: tjlu@mail.xjtu.edu.cn (T.J. Lu).

0266-3538/$ - see front matter © 2013 Elsevier Ltd. All rights reserved.
http://dx.doi.org/10.1016/j.compscitech.2013.07.011

corrugated cores were selected. In addition to experimental measurements, numerical investigations with the method of finite elements were also performed to reveal the interaction effects between the aluminum foam and the core members as well as the underlying mechanisms of enhanced strength and energy adsorption capability of the foam filled sandwich.

2. Fabrication methodology

Consider a sandwich panel having metallic foam-filled corrugated core, with both of its face sheets and core made of 304 stainless steel (density $\rho_s = 7900\ kg/m^3$). For reference, the sandwich panel with empty corrugated core was also considered. Fig. 1 shows schematically the fabrication processes for both empty corrugated panels and close-celled aluminum foam filled panels. The sandwich panel with empty corrugated core was produced by folding and laser welding technologies. Close-celled aluminum alloy foam fabricated via the melt foaming route in collaboration with the D.P. He Group of Southeast University, China, was used as the filling material [6]. Upon melting the Al alloy in a crucible, calcium particles were added as the adjuster to increase the viscosity of the melt. When the viscosity reached a proper value, titanium hydride powder as the blowing agent was added and dispersed in the melt. After a holding and cooling step, aluminum foam sheets with closed cells were obtained. Triangular foam prisms having the same shape of the core space of the corrugated core were subsequently cut by electro-discharge marching (EDM) from the aluminum foam sheet as the filling material. The triangular foam prisms were inserted into the corrugated core and fixed by using epoxy glue. Before assembling, surface cleaning was applied to both the empty sandwich panel and the foam prisms. The foam-filled panel was hold at 25 °C for 4 h, heated up to 80 °C for 2 h, and then cooled to ambient temperature (Fig. 1). The close-celled aluminum foam chosen for the present study had three different densities of $\rho_f = 297$, 432 and 540 kg/m^3, with an average cell size of ~2 mm; see Table 1. Note that the cellular morphologies and mechanical properties of the aluminum foam used in the present study were similar to the commercially available alporas foams (Shinko Wire Ltd., Japan) that had been investigated extensively, as both were processed with the essentially same method.

In the present study, to demonstrate the concept and the effect of inserting aluminum foam into the interstices of metallic sandwich plates with corrugated cores, stainless steel was selected although other metallic materials such as aluminum alloy, plain steel and titanium can also be used (which will be investigated in a separate study). Conventionally, the connection of dense metallic face sheet/core web and metallic foam is adhesive bonding [9]. However, due to manufacturing advantages and economical consideration, epoxy glue was selected in the present study. Further, besides the enhanced mechanical properties of the hybrid sandwich due to foam filling, the novel structure is also expected to possess good corrosion resistance, as it has been demonstrated that the adding of alloying element such as magnesium [19] and covering of coatings such as Ni–P [20] led to significantly improved corrosion resistance of the aluminum foam.

Fig. 2a displays the geometric parameters of a unit cell for the empty corrugated sandwich panel, whilst Fig. 2c shows a typical specimen for out of plane quasi-static compressive test, with fixed inclination angle ($\alpha = 45°$), core height ($H = 17$ mm), face sheet thickness ($h = 1.42$ mm), core member thickness ($t = 1.5$ mm) and width ($B = 20$ mm). To minimize boundary effects, specimens having three unit cells were employed in the tests. Fig. 2d shows a typical example of the as-fabricated sandwich panel filled with aluminum foam. With the densities of steel and aluminum foam denoted separately by ρ_s and ρ_f, the average density of the core ρ_c was defined as:

$$\rho_c = v_s\rho_s + \rho_f(1 - v_s) \tag{1}$$

where v_s is the volume proportion of the core occupied by the steel which is [17]:

$$v_s = \frac{t/H}{t/H + cos\alpha} \tag{2}$$

For empty corrugated sandwiches, $\rho_f = 0$, whilst for foam-cored sandwiches, $v_s = 0$. It should be further mentioned that, as impaired bonding condition between the foam and the core web may reduce the loading-carrying and energy absorption capability of foam-filled sandwich panels, the interface was treated carefully to minimize the clearance before epoxy glue was applied to fill the gaps. A typical image of the interface between foam and core web is presented in Fig. 2b, which shows in general good bonding condition has been achieved.

3. Experimental measurements and results

3.1. Experimental measurements

Quasi-static out-of-plane compression tests upon empty and foam-filled sandwiches as well as aluminum foam specimens were carried out with a hydraulic testing machine (MTS) at ambient temperature. A nominal strain rate of $10^{-3}\ s^{-1}$ was employed in all tests. At least 58% deformation in strain was achieved for each specimen to ensure full contact between core members and face sheets in an empty panel and to enable foam densification in a

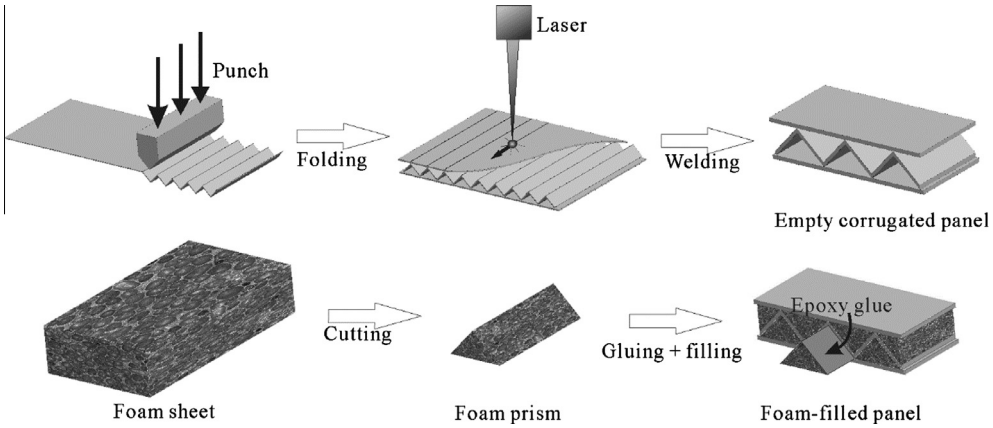

Fig. 1. Schematic of the fabrication process for sandwich panels having empty corrugated cores and aluminum foam-filled corrugated cores.

Table 1
Compressive peak strength and absorbed energy of empty and foam-filled sandwich panel with corrugated cores as well as aluminum foams. Each data in the table was the average of at least three specimens. A, B and C denote aluminum foams having different densities.

Properties	Aluminum foam			Empty panel	Foam-filled panel		
	A	B	C		A	B	C
ρ_c (kg/m^3)	297	432	540	869	1106	1264	1343
σ_{33}^{Peak} (MPa)	2.38	5.41	9.50	13.4	25.6	31.5	41.7
$\sigma_{33}^{Peak}/(\sigma_y\rho_c/\rho_s)$	0.30	0.47	0.66	0.58	0.85	0.95	1.16
W_v (10^3 kJ/m^3)	1.17	2.53	4.59	4.71	11.81	14.82	18.79
W_m (kJ/kg)	3.94	5.86	8.50	5.42	10.42	11.72	13.92

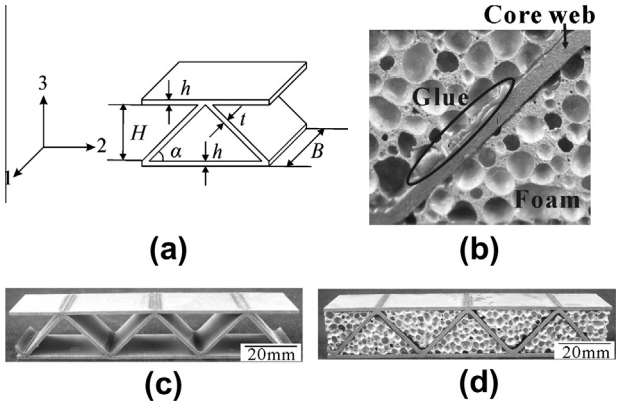

Fig. 2. Metal sandwich panel with corrugated core: (a) schematic of unit cell; (b) interface between foam and core web showing good bonding condition; (c) unfilled; (d) filled with aluminum foam.

foam-filled panel. No breakage of the welded joints was observed during the tests. Digital images of each sample were acquired by video camera.

3.2. Experimental results and discussion

The measured uniaxial compressive stress versus strain responses of a foam filled sandwich panel (curve A) and an empty panel (i.e., without foam filler and denoted by curve B) were shown in Fig. 3. For reference, the compressive stress versus strain curve of the aluminum foam used as the filler was also included (curve C). It was seen from Fig. 3 that the foam filled sandwich panel had much improved strength and plateau stress compared to the sum of those of the empty panel and the Al foam alone (the sum was represented by curve "B + C" in Fig. 3).

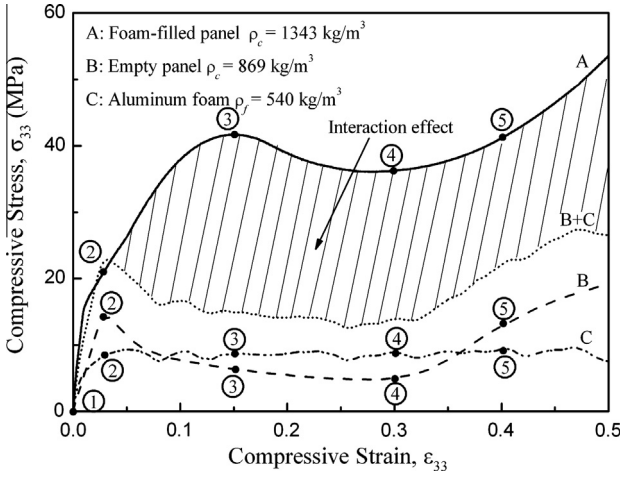

Fig. 3. Nominal stress versus strain curves of aluminum foam, empty panel and foam filled panel under compression.

The deformed configurations corresponding to points ①–⑤ marked on the stress versus strain curves of the empty panel, foam filled panel and Al foam in Fig. 3 were shown in Fig. 4a–c, respectively. As shown in Fig. 4b for the foam filled panel, foam filling had the effect of stabilizing core member buckling, resulting in much enhanced compressive strength relative to the empty panel. The most notable features were as follows: (i) Following the initial linear elastic response at low strains, the compressive stress increased nonlinearly, peaking at the strain of about 0.15 (Fig. 3). This strain corresponding to the peak stress was much larger than that of either aluminum foam or empty panel, indicating that the formation of plastic hinges in the foam-filled panel was significantly delayed as a result of the lateral support provided by the foam to the core members against plastic buckling. (ii) The peak

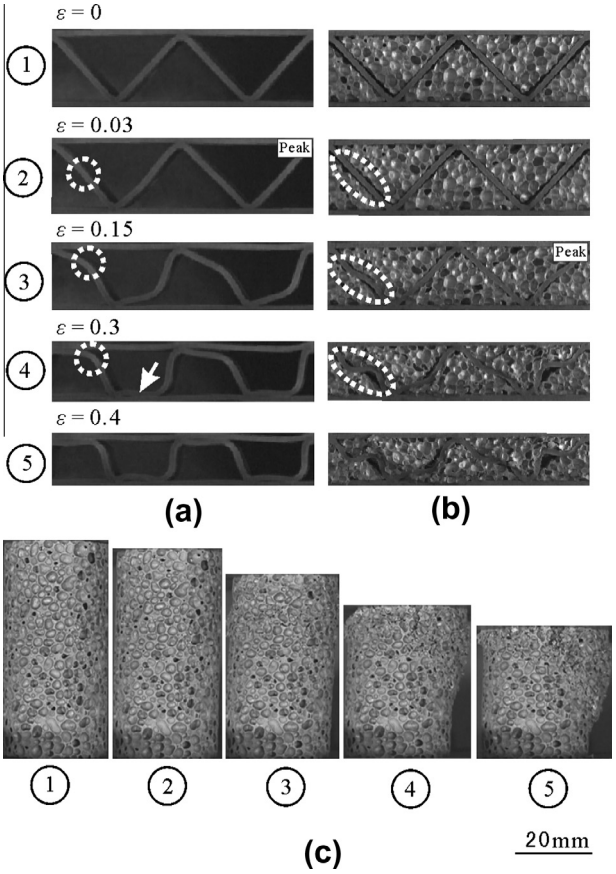

Fig. 4. Photographs illustrating the deformation history at selected points marked in Fig. 3: (a) empty panel, ρ_c = 869 kg/m^3; (b) foam-filled panel, ρ_c = 1343 kg/m^3; (c) aluminum foam, ρ_f = 540 kg/m^3. Arrow: contact between core member and face sheet. Circle and ellipse in dashed line: the evolvement of plastic hinges.

stress σ_{33}^{Peak} (~42 MPa) was considerably larger than the sum (~23 MPa, curve B + C, Fig. 3) of the aluminum foam and the empty panel tested separately, which was previously not achieved by filling the empty panel with structural polymeric foams [17,18]. (iii) As the strain was increased beyond that corresponding to the peak stress, the foam-filled core only slightly softened, in contrast to sudden dramatic stress drop of the empty corrugated core, indicating stabilized plastic buckling of the core members in the former. Instead of only one plastic hinge formed in each core member of the empty panel (Fig. 4a), at least two plastic hinges were formed in each core member of the foam-filled panel (Fig. 4b, ellipses in dashed line). (iv) Concomitance with core softening when the strain reached about 0.3, local densification of the aluminum foam in the vicinity of the core members occurred, resulting in increased stress with further increase in strain (Fig. 3). In contrast to the empty panel, the deformed core members started to contact the face sheets (Fig. 4a, $\varepsilon_{33} = 0.3$, arrow), leading to rapid increase in stress upon further deformation. In comparison, as was seen in Fig. 4c, the layer by layer crushing of the aluminum foam generated a long stress plateau region, typical for metallic foams [21] and different from the foam-filled and empty panels.

The energy absorption capacity may be characterized by the area under the uniaxial compressive stress versus strain curve. The energy absorbed per unit volume, W_v, was defined as:

$$W_v = \int_0^{\bar{\varepsilon}} \sigma d\varepsilon \tag{3}$$

where $\bar{\varepsilon} = 0.5$ was adopted. In addition, as mass was critical for energy absorbers for weight sensitive applications, the specific absorbed energy (or, absorbed energy per unit mass) was another important parameter. The absorbed energy per unit mass, W_m, may be defined as:

$$W_m = W_v/\rho_c \tag{4}$$

where ρ_c was the average density calculated by Eq. (1). To further characterize the mechanical performance of the test specimens, the compressive peak strength σ_{33}^{Peak} was normalized by $\sigma_y\rho_c/\rho_s$, σ_y being the yield strength of 304 stainless steel.

The results for the absorbed energy per unit volume, absorbed energy per unit mass and the compressive peak strength were summarized in Table 1. It was seen from Table 1 that filling of aluminum foam into the empty sandwich panel could increase the compressive peak strength σ_{33}^{Peak} and the absorbed energy per unit volume W_v by 211% and 300%, respectively. However, given that foam filling also increased the total mass of the sandwich panel, the normalized peak strength $\sigma_{33}^{Peak}/(\sigma_y\rho_c/\rho_s)$ and the specific absorbed energy W_m were deemed more proper parameters to characterize the mechanical performance of the present test specimens. The results of Table 1 demonstrated that, relative to an empty sandwich, foam filling increased $\sigma_{33}^{Peak}/(\sigma_y\rho_c/\rho_s)$ and W_m by as large as 100% and 157%, respectively. The significant increase of strength and energy absorption are inspiring for weight sensitive applications.

Recall that previous studies found the compressive strength and energy absorption of polymeric foam filled sandwich structures were both almost the sum of the lattice core and the polymeric foam alone [17]. The effect of inserting polymeric foams had thus been deemed to be minor. However, the present experimental results presented in Table 1 and Fig. 4 clearly demonstrated that, by inserting aluminum foam into the corrugated core, the sandwich panel could have much improved properties such as strength and energy absorption. The improvement (see, e.g., the shadow area between Curve A and Curve "B + C" in Fig. 3) was believed to caused by the strong interaction effect between the aluminum foam and the core members. As polymeric foams were much weaker than metal foams, they may not be able to supply sufficient lateral support to the core members if filled into the core of sandwich panels, as confirmed by existing studies [17,18]. In other words, the interaction between the polymeric foam and the metallic core members was negligible. For aluminum foam-filled corrugated sandwich panels, the strengthening mechanisms may be similar to metal foam-filled tubes, i.e., the metal foam filling reduced the buckling wavelength in the tube [13,14]. In the section to follow, the strengthening mechanisms underlying the present aluminum foam-filled corrugated sandwich panels were explored further using finite element (FE) simulations.

4. Numerical investigation

4.1. FE simulation

4.1.1. Material properties

The core members of the corrugated panels (304 stainless steel) were modeled using the von Mises J2 flow elastoplastic theory, with Young's modulus $E_s = 210$ GPa, Poison ratio $v = 0.3$, and yield stress $\sigma_y = 210$ MPa. The quasi-static plastic hardening stress versus strain curve of the material taken from Stout and Follansbee [22] was used in the FE simulations.

The crushable foam constitutive model of Deshpande and Fleck [23] was employed for the aluminum foam and the associated material parameters were: Young's modulus $E_f = 2.61$ GPa, Poisson ratio $v_f = 0.3$, and plastic Poisson ratio $v_p = 0$. The stress versus strain curve obtained from uniaxial compression tests (e.g., Fig. 3, curve C) was adopted in the simulations.

4.1.2. Details and validation of FE model

Finite element simulations of both empty and Al foam-filled corrugated panels under quasi-static compression were performed using ABAQUS/Explicit. The geometrical parameters were the same as those of the experimental specimens (Fig. 2). The face sheets were modeled as rigid bodies since they are much stiffer than the core structures. Both the corrugated core members and the filled foam were meshed as plane strain elements (i.e., Element CPE4R in ABAQUS). An average element size of 1/10 of the thickness of the corrugated core member was employed for both the core member and the foam. A mesh size sensitivity study was conducted, revealing that further refining of the mesh had little influence on the numerical results. The face sheets, the core members, and the foam were assumed to be perfectly bonded together. With symmetry boundary conditions applied as shown in Fig. 5, displacement controlled quasi-static uniaxial compression in the 2-direction was applied to the top face sheet while the bottom face sheet was fixed. The strain rate effect of stainless steel or aluminum foam was not incorporated in the constitutive properties used in the FE model, thus the materials were assumed

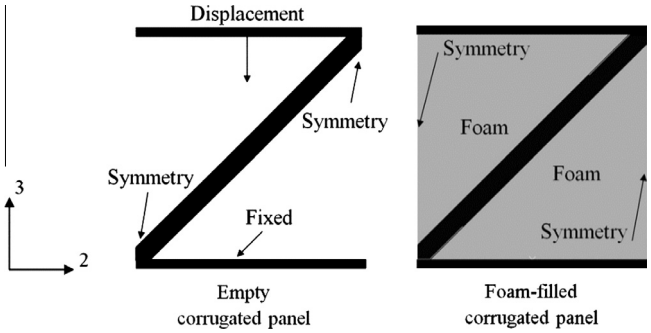

Fig. 5. Geometry and boundary conditions of FE model.

to be rate-independent. The loading speed imposed on the top face sheet of the panel was fixed at 0.06 s^{-1}, which was sufficiently low that the strain rate sensitivity of the constituting materials as well as the inertia effect may be disregarded. It has been further established (results not shown here for brevity) that, at this loading speed, the kinetic energy acquired by both the empty and the foam-filled panels was negligibly small compared to the plastic dissipation, suggesting that the whole crushing process may be treated as quasi-static.

In general, geometrical imperfections were inevitable in sandwich structures with lattice cores such as corrugated core and truss core. However, due to the low length-thickness ratio of the core member studied here, very good agreement between the experimental and FE results (assuming perfect bonding) was achieved even without considering any geometrical imperfections (Fig. 6). Therefore the influence of geometrical imperfections was neglected in the present study.

To investigate the influence of interfacial bonding condition between stainless steel and aluminum foam on the peak load and energy absorption, FE simulations for foam-filled sandwich panel having unbonded interfaces were carried out, and the results are shown in Fig. 6. As expected, the stress versus strain curve of the unbonded one is significantly lower than the perfect bonded one. It is also seen from Fig. 6 that the simulated results with perfect bonding assumed matched better with experimental measurements, indicating the use of epoxy glue provides nearly perfect bonding between aluminum foam and stainless steel (see Fig. 2b). Although debonding was observed when large plastic deformation occurred as the compressive strain exceeded 0.3, all subsequent FE simulations were based on perfect bonded interfaces as the present mechanism analysis aimed to focus on the early stage of deformation (compressive strain not exceeding 0.3). The influence of debonding was therefore not further considered.

It should be mentioned that the experimental results in Fig. 6 are only from one specimen. In reality, at least three sets of nominally identical specimens were used (see Table 1), including the foam itself, the empty panel and the filled panel (for each fixed foam density). It has been established that the results from nominally identical specimens agreed well. Consequently, in order to make Fig. 6 more clear and concise, we only choose one specimen to represent.

Additional calculations using three-dimensional (3D) elements were conducted, showing that the two-dimensional (2D) plane strain simulations provided slightly stiffer stress–strain responses. Nevertheless, the computationally much less demanding 2D simulations could capture the strength and deformation modes observed in the experiments with reasonable accuracy, as shown in Fig. 6. Most importantly, the exceptional strengthening phenomena and deformation modes of the foam-filled panels observed in the experiments were evidently predicted using this 2D model. Therefore, the 2D model was employed in the following simulations.

4.2. The mechanism of the strengthening effect of foam-filled panel

4.2.1. Deflection profiles of core members

The deflected profiles of the core members (i.e., struts) in both the empty panel and the foam-filled panel were plotted separately in Fig. 7a and b for different overall compressive strains. Significant difference could be seen between the strut deformation modes of the empty panel (Fig. 7a) and those of the foam-filled panel (Fig. 7b). Note that although the geometry and the loading condition were symmetric about the strut center for both the empty and foam-filled panels, the final deformation was not symmetric. The asymmetric deformation was triggered by the numerical round-off introduced in the explicit calculation, which played a similar role as an initial geometrical imperfection.

In the empty panel, only one dominant wavelet was observed along the deflected strut and the wave length almost covered the whole span of the strut. For the foam-filled panel under compression, however, four apparent wavelets with much smaller wave lengths were observed along the deflected strut (Fig. 7b). In addition, a comparison of Fig. 7a and b revealed that the maximum strut deflection of the empty panel was always larger than that of the foam-filled panel. For example, at $\varepsilon_{33} = 0.05$, the maximum strut deflection of the empty panel reached nearly 0.07L, as opposed to 0.001L for the foam-filled panel. Therefore, filling foam in the empty panel changed considerably the response of the inclined strut, including the number of wavelets as well as maximum strut deflection, both of which relevant to the overall compressive behavior of foam-filled corrugated panels.

4.2.2. Axial compressive stress across core member sections at plastic hinges

The axial stresses at different points across selected transverse sections of the strut as shown in the insert of Fig. 8 were investigated, with points A, B and C denoting separately the points at the concave end, at the center, and at the convex end of the chosen section. The axial stress, $-\sigma_{\xi\xi}$, normalized by the yield stress of the steel, σ_y, at each point as a function of the overall compressive strain of the sandwich panel, ε_{33}, was plotted in Fig. 8a. It should be pointed out that a point with positive stress underwent compression while negative stress represented tension.

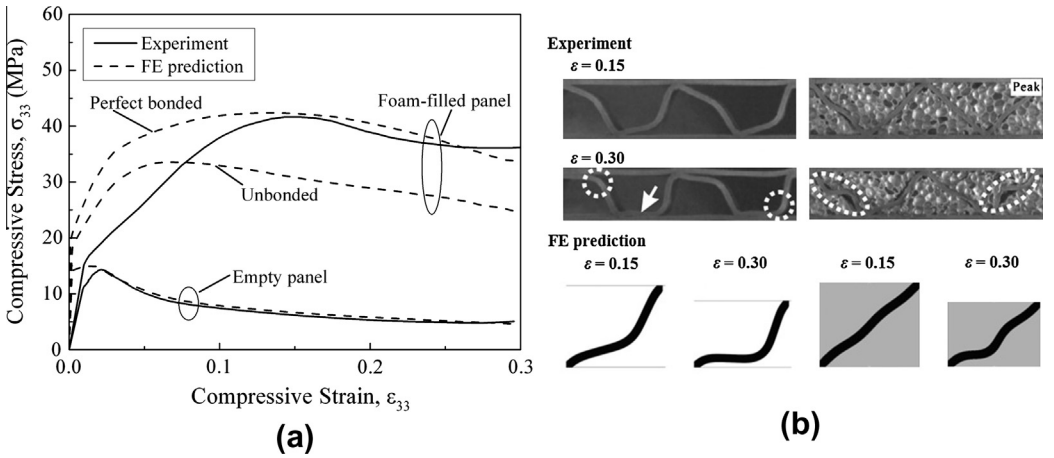

Fig. 6. Comparison of FE predictions with experimental measurements: (a) compressive stress versus strain curves, and (b) deformation modes, with $\rho_f = 540$ kg/m^3.

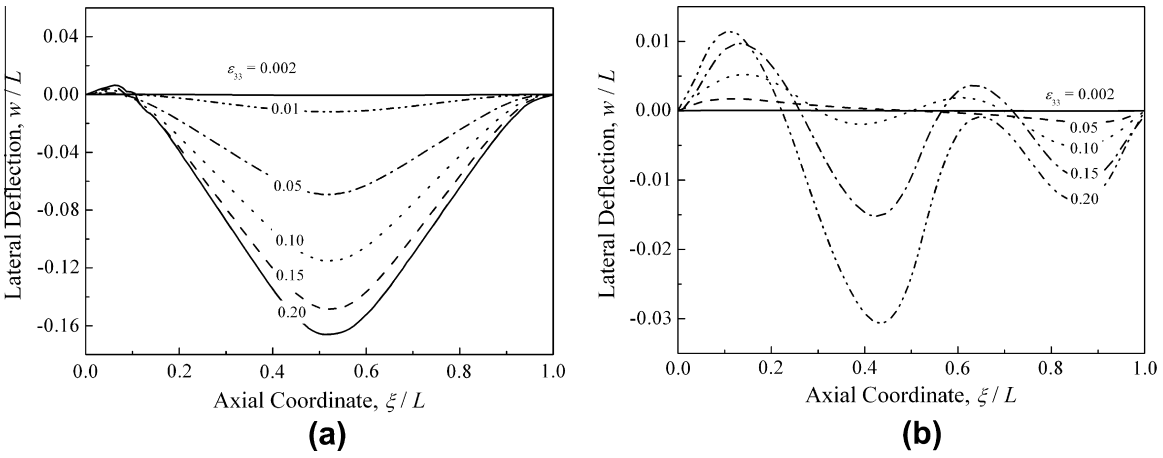

Fig. 7. Lateral strut deflection at different overall compressive strains in (a) empty panel and (b) foam filled panel.

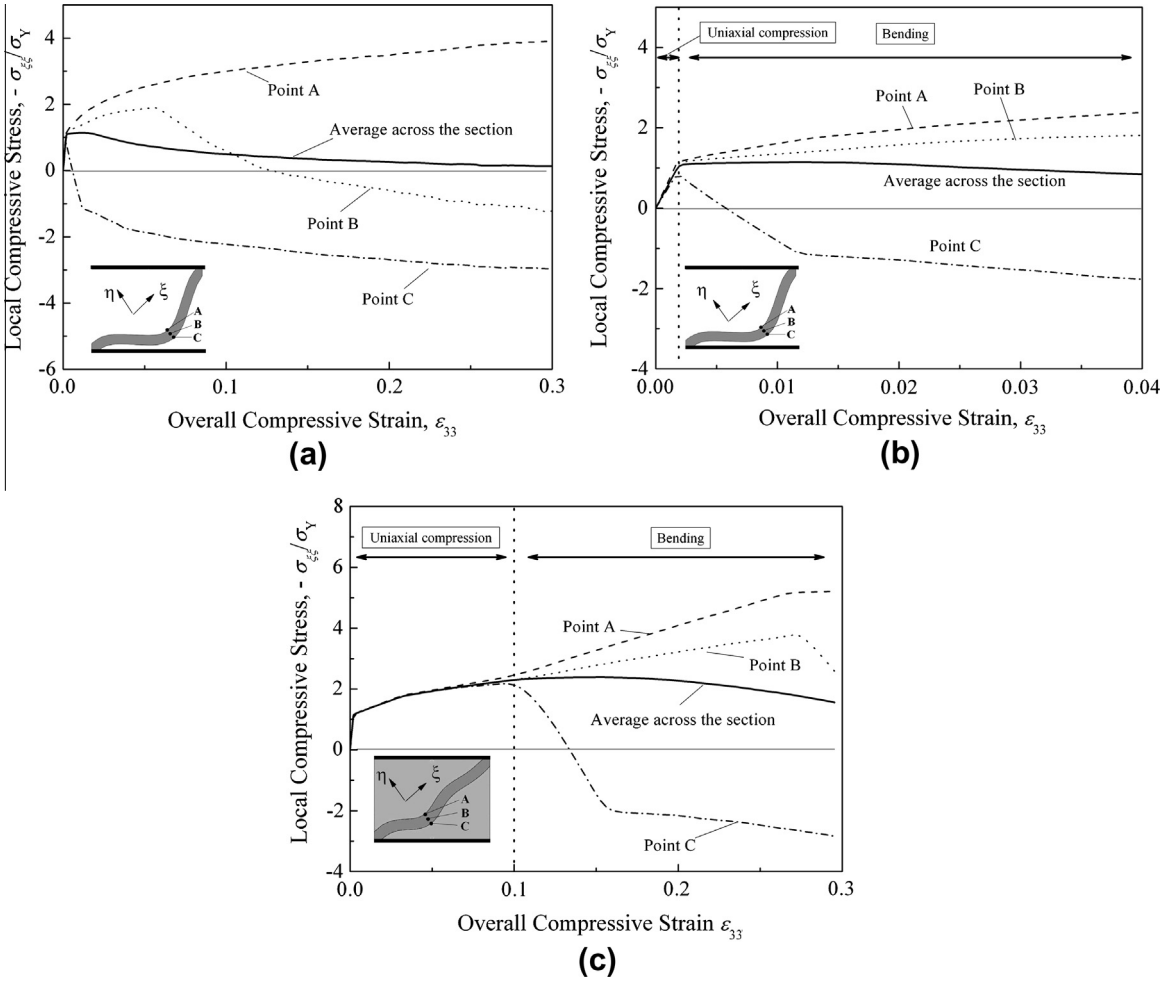

Fig. 8. History of axial stress at different points across the transverse section in the center of a plastic hinge of the strut in: (a and b) empty panel; (c) foam-filled panel.

For both the empty and foam filled panels, the strut first underwent axial compression during which the axial stresses at points A, B and C coincided. Subsequently, the strut started to deflect laterally (i.e., bending began to occur). When the panel was further compressed, the axial stresses at different points across the section diverged, indicating that bending started to prevail. The duration of the axial compression state of the strut was crucial for the strength of either the empty or the foam-filled panel. In the case of an empty panel, switching from axial compression to bending of the strut began as soon as the yield point was reached (about $\varepsilon_{33} = 0.002$). In the case of a foam-filled panel, however, the strut still experienced axial compression until $\varepsilon_{33} = 0.1$, beyond initial plastic yielding. Its load carrying capacity kept increasing due to the hardening properties of the stainless steel. When the strut deformation was dominated by lateral bending rather than axial compression, the compressive stress was gradually released and finally replaced with tensile stress, i.e., elastic unloading took place. When the unloading region became larger, the load carrying

capacity of the strut gradually decreased. It could be seen that elastic unloading at the points across the selected strut section of the foam-filled panel was significantly delayed compared to the empty panel, which indicated that lateral deflection of the strut was more difficult to develop in the foam-filled panel due to the constraints on the core member by the filled Al foam. Because the strut deflection of the foam-filled panel was much less than that of the empty panel, the drop of the load carrying capacity of the filled panel was not as dramatic as that of the empty panel (see, e.g., Fig. 3).

It should be mentioned that, in Fig. 8, perfect bonding between aluminum foam and stainless steel has been assumed which led to good agreement between FE simulation results and experimental measurements if the compressive strain did not exceed 0.3 (see Fig. 2a). However, for the present specimens, debonding did occur during experiment if the applied strain exceeded 0.3, and hence it would be interesting to explore how debodning may affect the peak load and energy absorption of the hybrid sandwich. This issue will be addressed in a future study.

5. Conclusion

Close-celled aluminum foam filled corrugated core sandwich panels made of stainless steel were fabricated and tested under uniaxial compression. It was found that the foam filling into the core of an empty corrugated sandwich could increase the compressive strength and energy absorption capacity of the hybrid sandwich by as much as 211% and 300%, respectively, and the specific energy absorption by 157%. The mechanisms underlying the enhancement were explored both experimentally and numerically. The significant increase of the peak stress and energy absorption was attributed to the lateral support to the core member by foam filling, altering the deformation modes and considerably delaying core member buckling. With high specific strength and specific energy absorption, all-metallic sandwich panels filled with aluminum foams hold great potential as novel lightweight structural materials for a wide range of crushing and impulsive loading applications. Future studies are nonetheless needed to systematically explore the influences of several important parameters, such as foam relative density, core member aspect ratio, foam/core member connecting condition, and loading rate. Loading conditions other than uniform compression need also to be addressed, such as three-point bending and simple shear.

Acknowledgments

This work was supported by the National Basic Research Program of China (2011CB610305), the National Natural Science Foundation of China (11021202, 11072188 and 11102152), the National 111 Project of China (B06024), the Shaanxi Province 13115 Project, and the Fundamental Research Funds for Xi'an Jiaotong University (xjj2011007). Constructive discussion with Dr. B.C. Li regarding numerical simulations was appreciated.

References

[1] Cote F, Deshpande VS, Fleck NA, Evans AG. Int J Solids Struct 2006;43:6220.
[2] Wilbert A, Jang WY, Kyriakides S, Floccari JF. Int J Solids Struct 2011;48:803.
[3] Xiong J, Ma L, Pan S, Wu LZ, Papadopoulos J, Vaziri A. Acta Mater 2012;60:1455.
[4] Wadley HNG. Trans R Soc A 2006;364:31.
[5] Fan HL, Fang DN, Chen LM, Dai Z, Yang W. Compos Sci Technol 2009;69:2695.
[6] Yang DH, Hur BY, He DP, Yang SR. Mater Sci Eng A – Struct 2007;445:415.
[7] Banhart J. Prog Mater Sci 2001;46:559.
[8] Crupi V, Montanini R. Int J Impact Eng 2007;34:509.
[9] Styles M, Compston P, Kalyanasundaram S. Compos Struct 2007;80:532.
[10] Idris MI, Vodenitcharova T, Hoffman M. Mater Sci Eng A – Struct 2009;517:37.
[11] Sun Z, Hu XZ, Sun SY, Chen HR. Compos Sci Technol 2013;77:14.
[12] Jeon I, Asahina T. Acta Mater 2005;53:3415.
[13] Zhang CJ, Feng Y, Zhang XB. Trans Nonferr Met Soc 2010;20:1380.
[14] Asavavisithchai S, Slater D, Kennedy AR. J Mater Sci 2004;39:7395.
[15] Chen WG, Wierzbicki T. Thin Wall Struct 2001;39:287.
[16] Nia AA, Sadeghi MZ. Mater Des 2010;31:1216.
[17] Vaziri A, Xue Z, Hutchinson JW. J Mech Mater Struct 2006;1:97.
[18] Burlayenko VN, Sadowski T. Compos Struct 2010;92:2890.
[19] Zhang YM, Chu XM, Wang H, He SY, He DP. Corros Sci 2009;51:1436.
[20] Liu JA, Zhu XY, Sudagar J, Diao W, Yu SR. Mater Trans 2011;52:2282.
[21] Gibson LJ, Ashby MF. Cellular Solids: Structure and Properties. second ed. Cambridge: Cambridge University Press; 1997.
[22] Stout MG, Follansbee PS. J Eng Mater – T Asme 1986;108:344.
[23] Deshpande VS, Fleck NA. J Mech Phys Solids 2000;48:1253.